Cellular Microbiology (2008) **10**(6), 1373–1389
doi:10.1111/j.1462-5822.2008.01134.x
First published online 12 March 2008

Calcium-binding protein 1 of *Entamoeba histolytica* transiently associates with phagocytic cups in a calcium-independent manner

Ruchi Jain,[1] Julien Santi-Rocca,[2,3] Narendra Padhan,[1] Sudha Bhattacharya,[4] Nancy Guillen[2,3] and Alok Bhattacharya[1]*
[1]*School of Life Sciences, Jawaharlal Nehru University, New Delhi, India.*
[2]*Institut Pasteur, Unité de Biologie Cellulaire du Parasitisme, Paris, France.*
[3]*INSERM, U786, Paris, France.*
[4]*School of Environmental Sciences, Jawaharlal Nehru University, New Delhi, India.*

Summary

EhCaBP1, a calcium-binding protein of the parasite *Entamoeba histolytica*, is known to participate in cellular processes involving actin filaments. This may be due to its direct interaction with actin. In order to understand the kinetics of EhCaBP1 in such processes, its movement was studied in living cells expressing GFP-EhCaBP1. The results showed that EhCaBP1 accumulated at phagocytic cups and pseudopods transiently. The time taken for appearance and disappearance of EhCaBP1 was found to be around 12 s. Site-directed mutagenesis was used to generate an EhCaBP1 mutant with reduced Ca^{2+}- and G-actin binding ability without any defect in its ability to bind F-actin. The overexpression of this mutant EhCaBP1 in the *E. histolytica* trophozoites resulted in the impairment of erythrophagocytosis, uptake of bacterial cells, killing of target cells but not fluid-phase pinocytosis. However, the mutant protein was still found to transiently localize with F-actin at the phagocytic cups and pseudopods. The mutant protein displayed reduced ability to activate endogenous kinase(s) suggesting that phagosome formation may require Ca^{2+}-EhCaBP1 transducing downstream signalling but initiation of phagocytosis may be independent of its intrinsic ability to bind Ca^{2+}. The results suggest a dynamic association of EhCaBP1 with F-actin-mediated processes.

Received 20 November, 2007; revised 30 January, 2008; accepted 16 February, 2008. *For correspondence. E-mail alok0200@mail.jnu.ac.in, alok.bhattacharya@gmail.com; Tel. (+91) 11 2670 4516; Fax (+91) 11 2671 7586.

Introduction

The enteric protozoan parasite *Entamoeba histolytica* is the causative agent of amoebiasis, an endemic disease in developing countries causing morbidity and mortality amongst large number of individuals (WHO/PAHO/UNESCO report, 1997; Stanley, 2003). All infected individuals do not develop invasive disease. It is not yet clear which factors are involved in transforming the commensal organism to an invasive virulent one in some individuals. Some of the early reports suggest that calcium (Ca^{2+}) signalling may have a role in the pathogenesis of amoebiasis (Ravdin *et al.*, 1982; 1985; 1988). The virulence of this organism is reflected in its capacity to invade human tissues and to phagocytose erythrocytes, bacteria and epithelial cells. The invasive process, pivotal for pathogenesis, is driven by motility of the parasite. Cell polarization is essential for the motility and results in the formation of a leading edge of the cell called pseudopod. Motility, as defined by amoeboid crawling activity, can essentially be divided into three different stages: pseudopod protrusion, pseudopod persistence and cell retraction. Pseudopods are also extended during phagocytosis of bacteria or human cells by *E. histolytica*. Precise spatial and temporal balance of the polymerized and unpolymerized pools of actin cytoskeleton is a key to production of pseudopods. Ca^{2+} is a prominent regulator that can exert multiple effects on the structure and dynamics of the actin cytoskeleton as shown in case of annexins (Gerke *et al.*, 2005).

It is clear from genome analysis that *E. histolytica* encodes a large number of calcium-binding proteins (CaBPs, Bhattacharya *et al.*, 2006). Majority of these proteins are unique to this organism as no homologues can be identified in other eukaryotes. This indicates that *E. histolytica* may possess extensive Ca^{2+} signalling pathways. However, in *E. histolytica*, only a few Ca^{2+}-mediated events have been described. Fibronectin-mediated adhesion (Carbajal *et al.*, 1996) and protein kinase C relocation from the cytosol to the membrane (De Meester *et al.*, 1990) are some of the processes where Ca^{2+} plays a critical role. Our main interest is to understand the role of EhCaBPs in the life cycle and virulence pathways of *E. histolytica*. EhCaBP1, previously identified from our laboratory, is a 14.7 kDa (134 amino acid

residues) protein, which shares low (29%) sequence identity with the well-studied eukaryotic EF hand-containing protein, calmodulin (CaM) (Prasad *et al*., 1992). The three-dimensional solution structure of holo-EhCaBP1 was determined by multidimensional nuclear magnetic resonance (NMR) spectroscopy (Sahu *et al*., 1999; Atreya *et al*., 2001) and X-ray crystallography (Gopal *et al*., 1998). Interestingly, NMR studies showed that EhCaBP1 has some structural similarity to CaM and TroponinC (TnC), with two globular domains connected by a flexible linker region spanning eight amino acid residues. Each domain consists of a pair of canonical Ca^{2+}-binding EF hand motifs. EhCaBP1 binds four Ca^{2+} ions with unequal affinity for Ca^{2+} (Gopal *et al*., 1997). However, differences exist which make EhCaBP1 distinct from CaM. Biochemically, the inability of EhCaBP1 to activate c-AMP phosphodiesterase differentiate it from all known CaMs (Yadava *et al*., 1997). Structural studies indicated a more open C-terminal domain for EhCaBP1 with larger water exposed total hydrophobic surface area as compared with CaM and TnC. Moreover, the central linker of EhCaBP1 contains two glycine residues (G63 and G67) making it more flexible compared with CaM. High-resolution X-ray crystallographic structure has recently been reported for EhCaBP1 (Kumar *et al*., 2007). The structure revealed an unusual arrangement of different domains not observed in previous studies. Unlike CaM, the first two EF hand motifs in EhCaBP1 are connected by a long helix and form a dumbbell-shaped structure. Three molecules of EhCaBP1 N-terminal domains participate in domain swapping to form trimers. The functional differences between EhCaBP1 and CaM could be attributed to the difference in the flexibility of the helices connecting the EF hand domains.

A decrease in the expression of EhCaBP1 gene in *E. histolytica* trophozoites by regulatable antisense RNA technology resulted in the inhibition of cellular proliferation, implicating the essentiality of the EhCaBP1 encoding gene in this parasite (Sahoo *et al*., 2003). Detailed analysis revealed that the defect in proliferation may be due to an inhibition of pinocytosis and phagocytosis and there was a direct interaction of EhCaBP1 with F-actin (Sahoo *et al*., 2004). Therefore it appeared that EhCaBP1 participated in processes involving actin skeletal dynamics and reduction in its cytosolic concentration could lead to a defect in actin-mediated processes, such as phagocytosis. Involvement of EhCaBP1 in phagocytosis was confirmed using phagocytosis-defective L6 mutant (Orozco *et al*., 1983). In these cells, EhCaBP1 expression was found to be highly reduced (Hirata *et al*., 2007). Phagocytosis plays an essential role in growth and constitutes one of the key virulence determinants of *E. histolytica* (Bracha and Mirelman, 1984).

Although EhCaBP1 localization to the pseudopods and involvement in phagocytosis has been reported, its kinetics in the process remains totally uncharacterized. As actin filament assembly is a dynamic process it is likely that EhCaBP1 may be involved in pseudopod formation during movement and phagocytosis in a transient manner. In the present work, multidimensional time-lapse imaging was used to study kinetics of EhCaBP1 in the live amoeba expressing EhCaBP1 tagged to GFP. The role of Ca^{2+} in the dynamics of EhCaBP1 was also investigated using a mutant form of EhCaBP1 having reduced ability to bind Ca^{2+}. The data highlight a very rapid kinetics of EhCaBP1 in the dynamic processes of pseudopod formation during parasite motility and phagocytosis. Reduction in the ability of EhCaBP1 to bind Ca^{2+} did not affect pseudopod formation at its early stages but altered a number of virulence properties of *E. histolytica* including red blood cell (RBC) phagocytosis and cell cytotoxicity. Analysis of phagocytic dynamic process revealed a dual behaviour of EhCaBP1. At early stages the interaction with filamentous actin, a step that does not require the Ca^{2+}-bound form of EhCaBP1, is important. In contrast, cytoskeleton dynamics during phagosome maturation requires EhCaBP1 to be in Ca^{2+}-bound state.

Results

Ca^{2+} requirement for phagocytosis in E. histolytica

It is known from many systems that Ca^{2+} is involved in phagocytosis (Lew *et al*., 1985; Stendahl *et al*., 1994; Vieira *et al*., 2002). To analyse the involvement of Ca^{2+} in phagocytosis of *E. histolytica*, human erythrocytes were used. The level of erythrophagocytosis was determined by a spectrophotometric assay after treating the trophozoites with different concentrations of the Ca^{2+} chelator, BAPTA-AM. The cells showed 60% reduction in the uptake of RBC at 50 μM of the chelator (Fig. 1). No significant effect was seen with DMSO, the solvent used to dissolve BAPTA-AM. Internal Ca^{2+} concentrations $[Ca^{2+}]_i$ was also determined. There was a 25% drop when the trophozoites were treated with 50 μM BAPTA-AM. This data suggest that $[Ca^{2+}]_i$ plays an important role in erythrophagocytosis.

Expression of GFP-EhCaBP1 in trophozoites

The cellular dynamics of any protein molecule can be studied in living cells by expressing the protein of interest tagged with GFP. In order to study the dynamics of EhCaBP1 in live trophozoites, GFP-EhCaBP1 was expressed in *E. histolytica* cells. The coding region of EhCaBP1 was inserted in frame into the BamHI site of *E. histolytica* shuttle plasmid pEh-NEO-GFP (Fig. 2A).

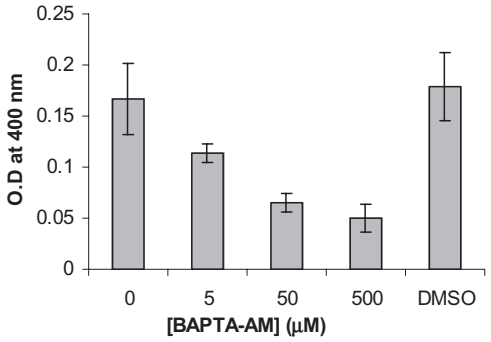

Fig. 1. Effect of calcium chelator BAPTA-AM on erythrophagocytosis in *E. histolytica*. The cells were grown for 48 h before treatment with different concentrations of BAPTA-AM (0 μM, 5 μM, 50 μM, 500 μM) or DMSO for 10 min at room temperature. Hundred thousand trophozoites were incubated with 10^7 RBC for 10 min followed by washing with chilled water to remove adhering cells. The amoebae with engulfed RBC were then lysed with formic acid. The data are presented as the amount of haem, determined by optical density at 400 nm ± SD for three separate experiments in triplicate.

E. histolytica cells were then transformed and stable transformants were selected as described in *Experimental procedures*. The cells carrying pEh-NEO-GFP-EhCaBP1 and the vector pEh-NEO-GFP plasmids will henceforth be referred to as GC1 and as GFP respectively.

Expression of GFP-EhCaBP1 from GC1 cells was studied by immunoblot analysis using anti-EhCaBP1 antibody and the results are shown in Fig. 2B. As the number of plasmids in transformed cells increases with increasing concentration of the selectable drug G418, the level of expression was determined at different concentration of the drug. The immunostained band for GFP-EhCaBP1 was seen at the expected size of 37 kDa and the intensity of the band increased with increasing concentration of G418 (Fig. 2B). The 14 kDa band represents the endogenous EhCaBP1 (Fig. 2B). Densitometric analysis of the blots revealed a threefold increase in the level of GFP-EhCaBP1 at 30 μg ml^{-1} G418 as compared with 1.5-fold at 10 μg ml^{-1} G418. The endogenous EhCaBP1 and actin showed no change in their levels at different G418 concentrations. In order to test if GFP-EhCaBP1 retains the properties of the endogenous EhCaBP1 *in vivo*, the property of the latter to localize at the phagocytic cup during erythrophagocytosis (Sahoo *et al*., 2004) was tested with the GFP-tagged protein. The localization of the fusion protein during erythrophagocytosis was studied by immunostaining with either anti-EhCaBP1 or anti-GFP antibodies. The cells showed an accumulation of GFP-EhCaBP1 in the phagocytic cups (Fig. 2D). The pattern was identical to that observed for endogenous wild-type (WT) EhCaBP1 (Fig. 2C and E) suggesting that GFP-EhCaBP1 behaves in a similar way as EhCaBP1 alone. The control GFP cells were also stained and the results showed that there is no accumulation of GFP at the phagocytic cup (Fig. 2F).

Dynamics of GFP-EhCaBP1 movement in live E. histolytica *cells*

Phagocytosis of particles is a rapid event in *E. histolytica* and closed phagosomes appear three minutes after the engulfment (Marion *et al*., 2005). The presence of EhCaBP1 in phagocytic cups suggested that it might be involved in the early stages of phagocytosis. In an attempt to examine the occurrence of EhCaBP1 on the mature phagosomes, the cells were stained for actin and EhCaBP1 after 10 min of erythrophagocytosis. As phagocytosis is not a synchronized event, it was possible to visualize cells undergoing phagocytic cup formation and also observe mature phagosomes. It was observed that F-actin was detached from the mature phagosomes (Voigt and Guillen, 1999). Focal planes in the middle of cells were analysed and engulfed RBC were seen inside the cells; however, neither actin nor EhCaBP1 was visible around the internalized RBC unlike EhCaBP1 colocalized with F-actin at the phagocytic cups (Fig. 3). These observations suggest that EhCaBP1 may be involved in phagocytosis only transiently at the initiation of the process and leaves the site during phagosome maturation. In order to further analyse this hypothesized dynamics of EhCaBP1 within the cell, GFP-EhCaBP1 trafficking was studied using multidimensional time-lapse fluorescence microscopy in GC1 cells. Video microscopy was carried out with spinning disk confocal scanning microscope in order to minimize damage to the cells due to laser energy and atmospheric oxygen and providing rapid acquisition of images. EhCaBP1 was found to move rapidly to and from the phagocytic cups. Live cell imaging of the GC1 cells in the presence of RBC showed that EhCaBP1 started to accumulate in the phagocytic cup as soon as the RBC bound to the amoeba surface. The intensity of EhCaBP1 increased rapidly during the uptake of RBC. There was a complete loss of fluorescence as soon as the RBC was completely inside the cell (Figs 3 and 4A). It took about 30 s from the appearance of EhCaBP1 to its eventual disappearance. Images from GFP cells were also captured but these showed a diffuse distribution of GFP alone (data not shown).

To gain insight in the dynamics of EhCaBP1, we took advantage of larger surface of pseudopods compared with those of phagocytic cups that have small areas. The acquired images are presented as fluorescent micrographs of a moving trophozoite taken every 3 s (Fig. 4B, see also Movie S1). A progressively marked enrichment of GFP-EhCaBP1 at the leading edge of the protruding pseudopods in comparison with cytoplasm and its subsequent disappearance was observed (Fig. 4B and C). The

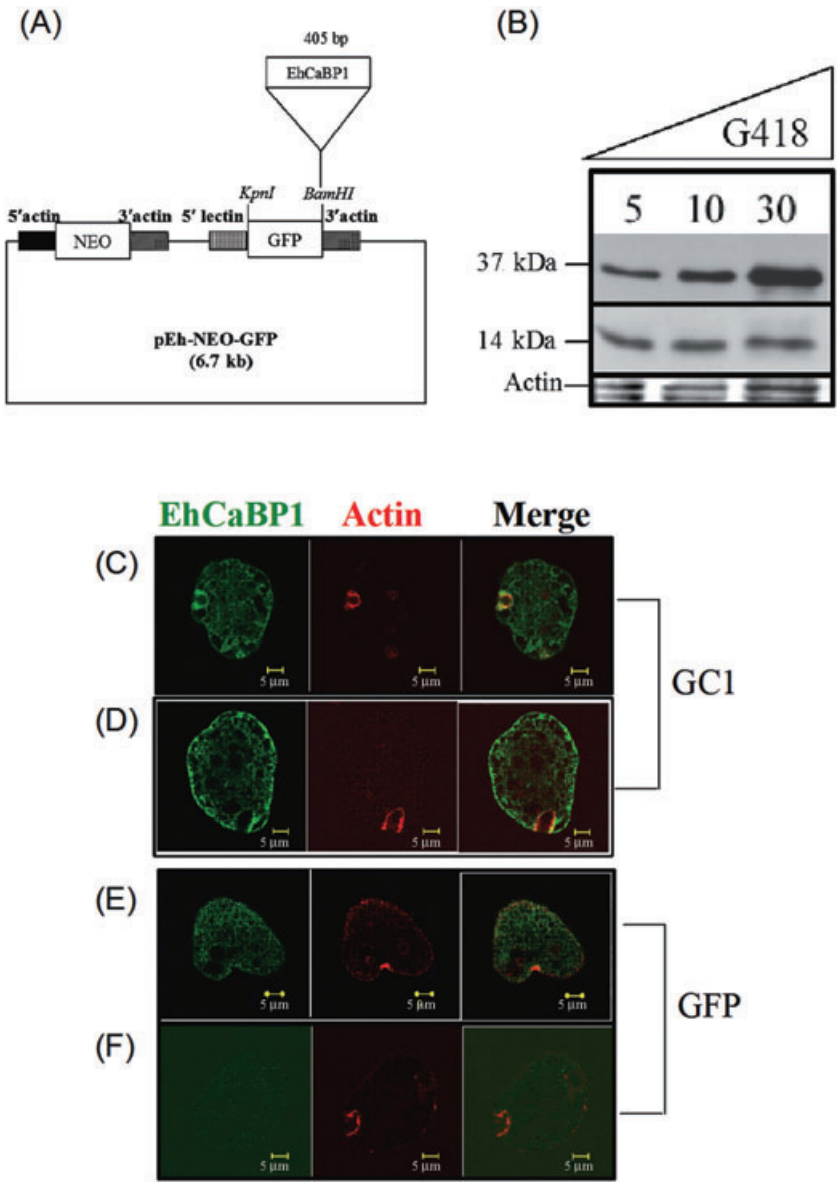

Fig. 2. Expression and immunolocalization of EhCaBP1-GFP in *E. histolytica*.
A. Schematic representation of GFP-EhCaBP1 (GC1) construct. EhCaBP1 gene (405 bp) was cloned in the BamHI site of pEh-NEO-GFP vector downstream from the GFP gene.
B. Immunoblot of the lysates of GC1-transfected cells at different G418 concentrations (5, 10, 30 µg ml^{-1}). Fifty micrograms of the lysate was loaded in each lane and probed with anti-EhCaBP1 antibody. The blots were stripped and re-probed with anti-Ehactin antibody. Anti-EhCaBP1 antibody stains both the endogenous EhCaBP1 band at 14 kDa and the GFP-fused EhCaBP1 band at 37 kDa.
C–F. Distribution of EhCaBP1 in GC1 or GFP cells during erythrophagocytosis. GC1 (C and D) and GFP (E and F) cells grown at 10 µg ml^{-1} G418 were incubated with RBC for 7 min followed by fixation and immunostaining. The cells were double-labelled for EhCaBP1 (C and E) or GFP (D and F) and F-actin (phalloidin red) and viewed using Confocal Scanning Laser Microscope. EhCaBP1 or GFP was visualized with green (Alexa-488) secondary antibody. Bars represent 5 µm.

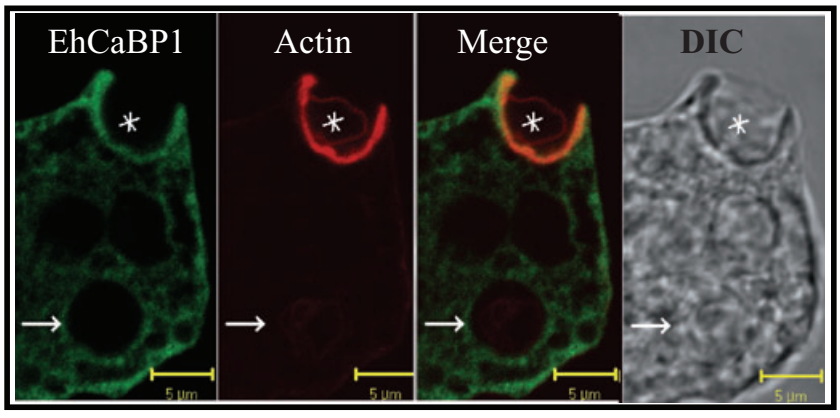

Fig. 3. EhCaBP1 immunostaining of phagosomes. Trophozoites grown for 48 h were transferred to pre-warmed, acetone-washed coverslips for 10 min at 37°C. The attached cells were further incubated with RBC for 10 min at 37°C. The cells were then fixed and immunostained with anti-EhCaBP1 antibody (green) and phalloidin (red). The focal planes of the cells having both phagosomes and phagocytic cups were viewed with Confocal Scanning Laser Microscope. The micrograph shows an optical section of one such representative cell. Bars represent 5 µm. Notice the recruitment of EhCaBP1 along with F-actin to the phagocytic cup (asterisk) and the disappearance of these markers from mature phagosomes (arrows).

image panel (Fig. 4C, left) clearly indicated that GFP-EhCaBP1 exhibited the highest degree of accumulation in fully formed pseudopods (Fig. 4C, ii) and rapid dissipation during retraction (Fig. 4C, iv). The result is also presented as a line scan (Fig. 4C, right), which exhibits changes in fluorescent intensity across a cell along a line. The line scan has been plotted for a pseudopod showing a cycle of projection and retraction of a representative cell.

Quantitative analysis of such pseudopods ($n = 30$) was carried out to determine the average time taken for EhCaBP1 molecule to be enriched within the pseudopods. Here, the amount of fluorescence in pseudopods was determined along a time kinetics. The fluorescence intensity increased as the pseudopod was formed and peaked at the time of protrusion (~6 s) (Fig. 4D) followed by a gradual decline of about 12 s. A decrease in the fluorescence was observed during retraction. The rate of loss of fluorescence was much slower than the rate of accumulation paralleling the formation and retraction of pseudopods.

It was also of interest to determine the fraction of total EhCaBP1 that may be present in a given pseudopod. In order to compute this, fluorescent intensity of protruded pseudopods was determined. Analysis of the data generated from 30 different pseudopods and cytoplasmic segments suggested that 12 ± 4% of the total cellular EhCaBP1 was present in a given pseudopod. Low level of fluorescent molecules in cytoplasm may reflect dilution of the label due to larger volume. The results suggest that EhCaBP1 is a highly dynamic molecule with a high rate of accumulation and disappearance from preferred sites.

Generation of mutant EhCaBP1

It is difficult to conclude from the previous results that Ca^{2+} binding is important for participation of EhCaBP1 in pseudopod extension during motility or phagocytosis as Ca^{2+} chelator would affect whole repertoire of EhCaBPs. EhCaBP1 possess four canonical EF hand Ca^{2+}-binding motifs, of which two display high affinities (Gopal *et al*., 1997). The role of Ca^{2+} in some of the activities of EhCaBP1 was investigated by generating point mutations. Point mutations were introduced by site-directed mutagenesis into each of the EF hands to disrupt the Ca^{2+} binding ability, while maintaining the overall structure of the domain. The first aspartate (D) residue of EF hand domains is one of the important residues involved in coordinating Ca^{2+} and mutating it affects Ca^{2+} binding (Geiser *et al*., 1991). Therefore, all the four D residues (10, 46, 85, 117) of EhCaBP1 EF hand domains were converted to alanine (A) singly or all at once. The mutants were named EFI, EFII, EFIII and EFIV, after the EF hand domain which was mutated. The mutant having the first D's of all four EF hands mutated to A was termed CaBP1ΔEF (Fig. 5A). The mutant proteins were expressed and purified from bacterial cells as described for the WT protein (Prasad *et al*., 1993). These mutants were tested for their Ca^{2+}-binding properties. As a first indication of the ability of the proteins to bind Ca^{2+} and undergo a conformational change, electrophoretic mobility in the presence of Ca^{2+} was checked by SDS-PAGE (Fig. 5B). The Ca^{2+}-bound form of EhCaBP1 undergoes a mobility shift in SDS-PAGE, reflecting Ca^{2+} binding and subsequent conformational change (Prasad *et al*., 1993). The single-point mutants showed a similar change in relative mobility of Ca^{2+}-free (EGTA) and Ca^{2+}-bound forms as the WT protein. In contrast, there was no difference in the mobility of the two forms in the case of CaBP1ΔEF, the mutant with all the four EF hands mutated.

It was shown before by CD spectroscopy that there is a major increase in helicity of EhCaBP1 on binding Ca^{2+}. This increase in helicity is reflected in a large change in conformation (Gopal *et al*., 1997). The variation in secondary structure of Ca^{2+}-bound form of mutant EhCaBP1s was also studied using CD spectroscopy (Fig. 5C). While two of the single mutants (EFI and EFIII) did not show much difference from the WT protein, some differences were observed for the other two (EFII and EFIV) mutants. On the other hand CD spectrum of CaBP1ΔEF protein suggested a molecule with low level of secondary structure, very different from the WT molecule. Moreover, no change in helicity was observed for CaBP1ΔEF in the presence or absence of Ca^{2+} (data not shown) in contrast to the WT EhCaBP1. These results suggest that either CaBP1ΔEF is unable to bind Ca^{2+} or it is defective in its ability to undergo Ca^{2+}-induced conformation change.

Isothermal calorimetry (ITC) has been frequently used to study Ca^{2+} and other metal ions interaction with proteins (Leavitt and Freire, 2001). It has also been used to study the thermodynamics of Ca^{2+} binding to EhCaBP1 (Gopal *et al*., 1997). Thus, in order to check if CaBP1ΔEF can bind Ca^{2+}, ITC was used (Fig. 6). The figure shows the integrated binding isotherms obtained after fitting to the best least square fit. WT EhCaBP1 was best fitted to the four site binding model while CaBP1ΔEF fitted to the single site binding model, indicating a major loss in Ca^{2+} binding sites. Loss of Ca^{2+} binding by the mutant protein was also confirmed by [^{45}Ca] binding assay in blots (data not shown here). The structural analysis suggests that CaBP1ΔEF is defective in Ca^{2+} binding and it has resulted in its inability to form secondary structure in the presence of Ca^{2+}. Therefore CaBP1ΔEF mutant was used for further functional study.

Characterization of the CaBP1ΔEF binding to G-actin and F-actin

The direct binding of EhCaBP1 to F-actin was previously demonstrated (Sahoo *et al*., 2004). It was also shown that

(A)

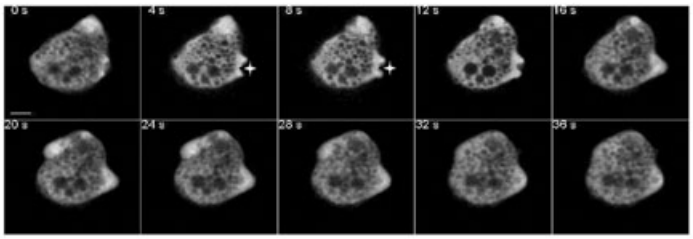

(B)

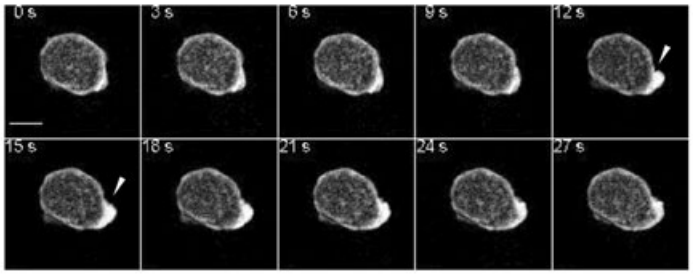

(C)

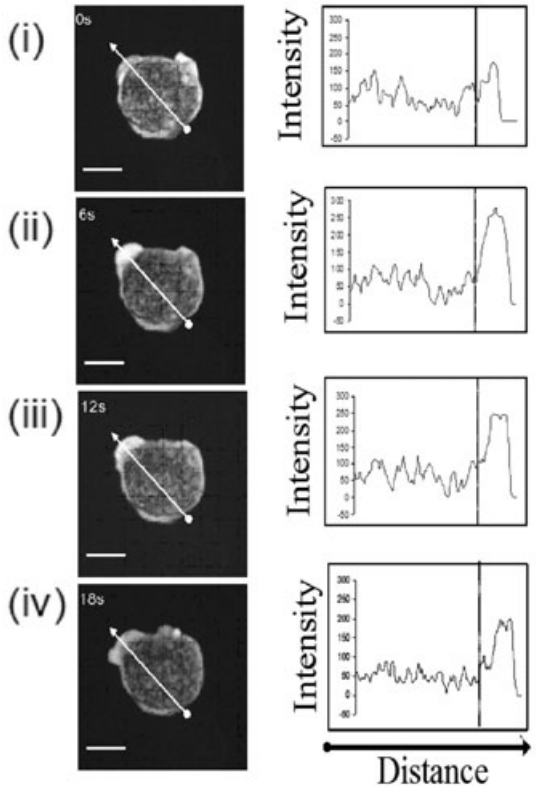

(D)

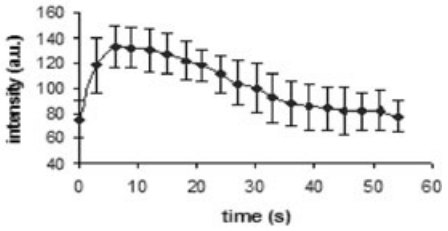

Fig. 4. Live cell time-lapse imaging of EhCaBP1.
A. Time-lapse micrographs during phagocytosis of RBC by an amoeba expressing GFP-EhCaBP1, showing *de novo* formation of a phagocytic cup. GC1 cells were mixed with RBC and then images of a stack of 15 sections along the z-axis (every 1.5 μm) were recorded every 4 s. Each stack of focal planes was projected after three-dimensional reconstruction as described in *Experimental procedures*. The montage shows a time series of a representative cell showing the formation of a phagocytic cup (star) and finally the closure of the phagocytic cup. Time is shown in seconds. Bar represents 5 μm.
B. The micrograph represents a time series of movement of a trophozoite expressing GFP-EhCaBP1. GC1 cells were allowed to attach to the culture dish and the images of the moving amoeba were captured using video microscopy. The images were recorded every 3 s, capturing a stack of 12 focal planes. The analysis and the three-dimensional reconstruction was performed as described in *Experimental procedures*. Arrowheads represent the images showing the protrusion of the pseudopod and the marked enrichment of GFP-EhCaBP1. Bar represents 10 μm.
C. Left: A representative cell, going through a cycle beginning with pseudopod protrusion (ii) and ending with retraction (iv), is shown. The fluorescent images were taken every 6 s. Right: The line intensity scan of the fluorescence intensity measured on the line overlaid on the corresponding images in left panel. Bars represent 10 μm.
D. Quantitative analysis of GFP-EhCaBP1 localization in the pseudopods. The graph presents the kinetics of movement of GFP-EhCaBP1 in the pseudopods of moving amoebae. The fluorescence intensity associated with the pseudopods was plotted against time in seconds. The data shown are the mean intensity ± SD from 30 different pseudopods.

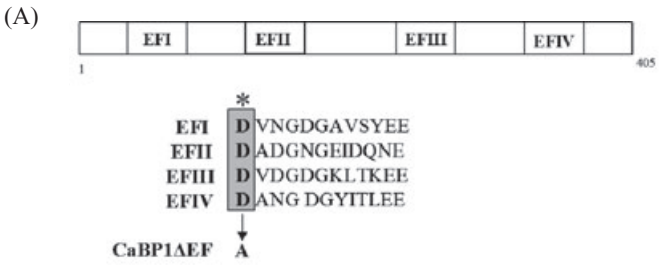

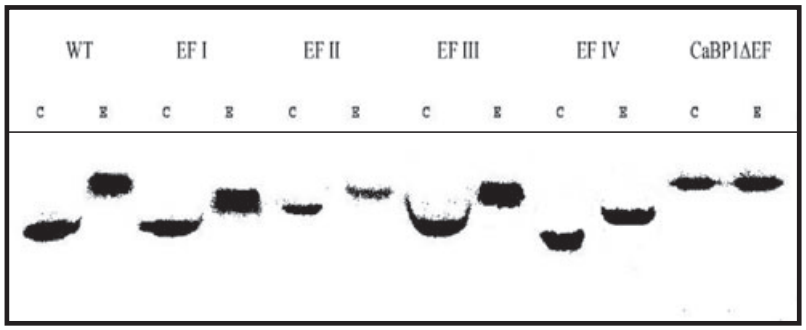

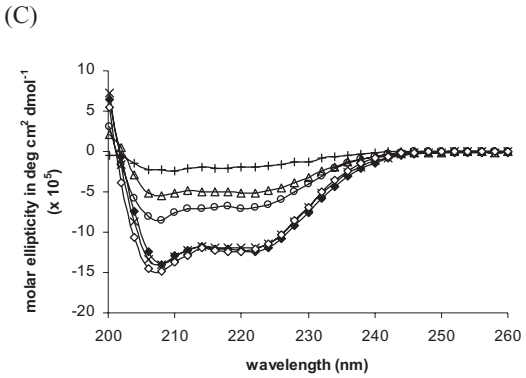

Fig. 5. Generation and characterization of EhCaBP1 mutants.
A. Schematic representation of EhCaBP1 indicating the four EF hand domains. The sequence of all the EF hands is shown and the first aspartate (D) of each EF hand was mutated to alanine (A) individually or simultaneously to generate EFI, II, III, IV or CaBP1ΔEF mutants respectively.
B. Gel mobility shift of Ca^{2+}-bound and Ca^{2+}-free forms of EhCaBP1 wild type (WT) and mutants. Recombinant proteins were purified from *E. coli* lysates expressing EhCaBP1 WT or mutants. Five micrograms of purified proteins (as indicated) were subjected to electrophoresis on a 15% SDS-PAGE in the presence of 5 mM Ca^{2+} (C) or 2 mM EGTA (E). The proteins were stained with Coomassie brilliant blue R-250.
C. CD spectrum of EhCaBP1 WT and mutants. The CD profiles of WT (◇), EFI (◆), EFII (Δ), EFIII (x), EFIV (○) and CaBP1ΔEF (+) in the presence of 50 mM Tris·Cl (pH 7.5), 100 mM NaCl and 5 mM $CaCl_2$ are shown.

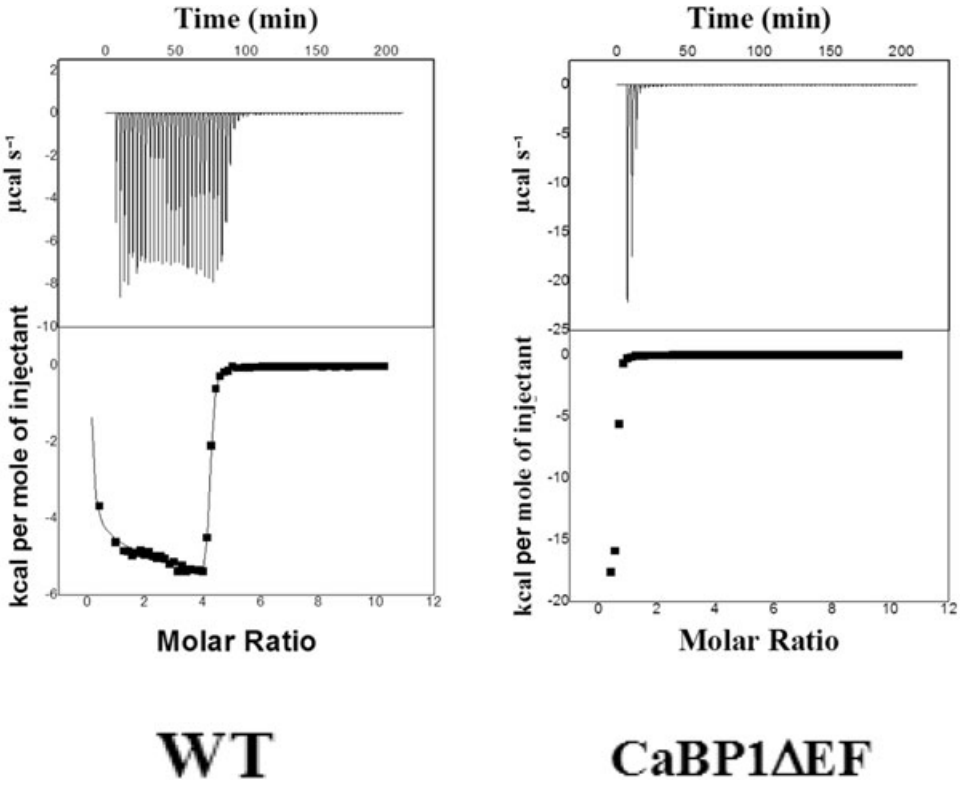

Fig. 6. Isothermal titration calorimetric analysis of Ca^{2+} binding to CaBP1ΔEF. Plot of kcal mol^{-1} of heat absorbed/released per injection of $CaCl_2$ as a function of molar ratio of Ca^{2+}:protein at 25°C is shown. Traces of the calorimetric titrations are shown at the top and the corresponding integrated binding isotherms shown at the bottom (solid lines represent the best least squares fit). EhCaBP1 (WT) fitted to the four sequential binding site model while CaBP1ΔEF fitted to one binding site model. For WT EhCaBP1, $K1 = 5 \times 10^3\ M^{-1}$, $\Delta H1 = -1.8 \times 10^3$ kcal mol^{-1}, $K2 = 1.4 \times 10^4\ M^{-1}$, $\Delta H2 = 2.3 \times 10^5$ kcal mol^{-1}, $K3 = 5.1 \times 10^5\ M^{-1}$, $\Delta H3 = -2.4 \times 10^5$ kcal mol^{-1} and $K4 = 1.5 \times 10^6\ M^{-1}$, $\Delta H4 = -7.9 \times 10^3$ kcal mol^{-1}. For CaBP1ΔEF, $K = 2.3 \times 10^6\ M^{-1}$, $\Delta H1 = -1.8 \times 10^4$ kcal mol^{-1}.

EhCaBP2, a homologue with 79% sequence identity, did not bind actin, suggesting that this interaction is highly specific. The ability of the CaBP1ΔEF mutant protein was also examined for the direct binding to F-actin using co-sedimentation assay. Purified CaBP1ΔEF was incubated with actin filaments and assessed for co-sedimentation at high speed. In the absence of actin, no CaBP1ΔEF was observed in the pellet (Fig. 7A, lane 4). However, on incubation with actin filaments CaBP1ΔEF was found in the pellet similar to EhCaBP1 (Fig. 7A, lane 2, 6). EhCaBP2 did not co-sediment with actin, as expected (Fig. 7A, lane 8). The direct interaction of CaBP1ΔEF with the actin filaments suggests that interaction with actin may not require either Ca^{2+} binding and or conformation transition.

To assess the binding of this mutant to G-actin, a solid-phase assay was carried out as described before for the WT protein (Sahoo *et al.*, 2004). Surprisingly, only 20% binding was observed in case of the mutant CaBP1ΔEF as compared with the WT EhCaBP1 suggesting that loss in Ca^{2+} binding leads to a reduction in the ability of EhCaBP1 to bind G-actin while retaining its ability to bind F-actin (Fig. 7B).

Properties of cells overexpressing CaBP1ΔEF

In order to understand the properties of CaBP1ΔEF, the construct was overexpressed with a GFP tag in the *Entamoeba* trophozoites. The same strategy was followed as for the WT GFP-EhCaBP1. The transfectants were maintained at 10 µg ml^{-1} G418. The overexpression was checked by immunoblotting (Fig. 8A) using anti-EhCaBP1 antibody. Densitometric analysis of the immunoblot showed a 2.5-fold increase in the expression of GFP-CaBP1ΔEF at 30 µg ml^{-1} G418 as compared with the cells maintained at 10 µg ml^{-1} G418.

Erythrophagocytosis

Erythrophagocytosis was initiated in the cell line expressing GFP-CaBP1ΔEF and the cells were then processed for immunolocalization (Fig. 8B). The confocal sections showed the presence of the mutant (stained with anti-GFP) protein at the phagocytic cup and its complete colocalization with F-actin in cells analysed at two different G418 concentrations (10 and 30 µg ml^{-1}). RBC were found to remain attached to the membrane and only a

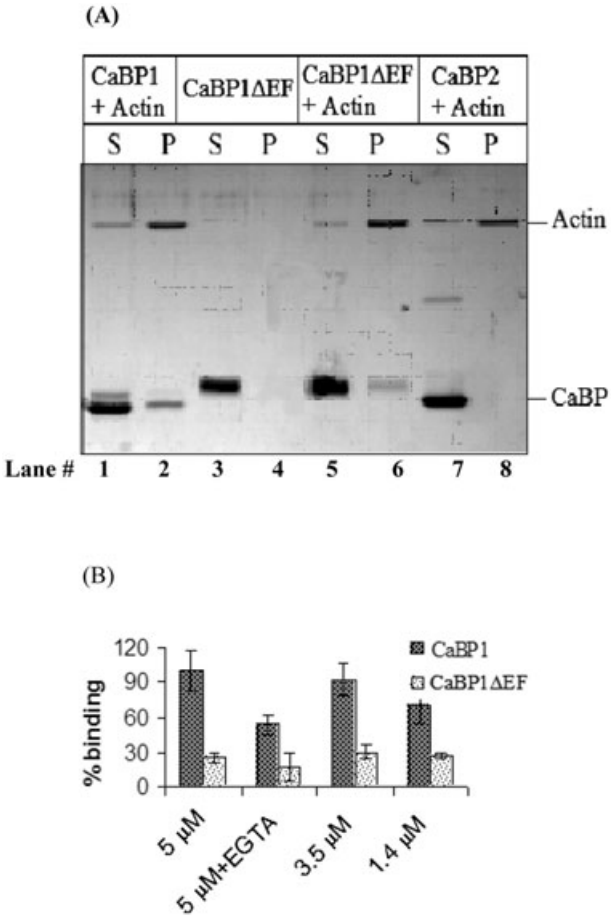

Fig. 7. Binding of CaBP1ΔEF to actin.
A. Co-sedimentation of CaBP1ΔEF with F-actin. Purified recombinant CaBP1ΔEF (5 μM, lanes 5, 6), EhCaBP1 (5 μM, lanes 1, 2) and EhCaBP2 (5 μM, lanes 7, 8) were incubated with polymerized actin (5 μM) in polymerization (G) buffer containing salts. CaBP1ΔEF was also incubated alone without actin (lane 3, 4). This was followed by ultra centrifugation to separate supernatant (S) and pellet (P) fractions. S (one-fourth of the total) and P (total) fractions were separated on a 15% SDS-PAGE followed by Coomassie blue staining.
B. Binding of CaBP1ΔEF to G-actin. Actin (5 μM) was coated on the microtitre plates overnight at 4°C. After blocking with BSA, CaBP1ΔEF and EhCaBP1 were added at the indicated concentrations in the presence of 5 mM $CaCl_2$ or 2 mM EGTA. This was followed by incubation with anti-EhCaBP1 antibody. The amount of bound EhCaBP1 was detected by using anti-rabbit IgG-HRPO. The amount of bound second antibody is determined by absorbance at 405 nm. The histogram shows the relative mean intensity ± SD of three independent experiments.

very few internalized RBC were observed at 30 μg ml^{-1} G418 suggesting a defect in the uptake of RBC. The level of erythrophagocytosis was also determined spectrophotometrically (Fig. 8D). RBC uptake was comparable in all the cell lines expressing GFP vector alone, GFP-EhCaBP1 or GFP-CaBP1ΔEF expressing cells at 10 μg ml^{-1} G418. However, at higher G418 concentration, a 60% reduction was observed in cells carrying GFP-CaBP1ΔEF (2.5-fold increased) confirming results obtained by confocal imaging. The data suggest that overexpression of a Ca^{2+}-insensitive form of EhCaBP1 leads to a dominant negative phenotype affecting late stages of phagosome maturation rather than early stages of phagocytosis.

Time-lapse microscopy was also used to determine the rate of appearance and disappearance of the mutant EhCaBP1 from the pseudopods. The results are shown as a micrograph of a representative cell (Fig. 8E). As described above for the WT protein, the mutant protein was also found to disappear from the pseudopods rapidly during retraction. The results suggest that the dynamic association of EhCaBP1 with actin-mediated processes, such as pseudopod formation, does not require Ca^{2+} binding.

Bacterial uptake and cytotoxicity

Both the properties, bacterial uptake and the ability to kill target cells, were found to be defective in cells overexpressing the mutant protein. Cytotoxicity was measured by the ability of *E. histolytica* cells to kill Chinese hamster ovary cells (CHO). The results are shown in Fig. 9A and B. As observed for the RBC uptake, the cells expressing GFP-CaBP1ΔEF at high levels showed a 70% reduction in their ability to destroy CHO monolayer (Fig. 9A) and also a 50% defect in bacterial uptake (Fig. 9B). No significant effect was observed for the parental cells or cells carrying vector alone.

Pinocytosis

Fluid-phase endocytosis was measured by determining the uptake of the fluorescent marker (RITC-dextran) by GFP, GC1 and GFP-CaBP1ΔEF cells. There was no significant difference observed for any of the transfectants under the assay conditions (Fig. 9C).

Reduced activation of kinase by mutant EhCaBP1

The decrease in the RBC uptake by the cells overexpressing the Ca^{2+}-insensitive EhCaBP1 suggested that Ca^{2+}-bound form of EhCaBP1 may be responsible for initiating downstream signalling leading to phagosome formation. As it is known that EhCaBP1 can activate specific kinase(s), the ability of CaBP1ΔEF to activate endogenous kinase(s) was investigated (Yadava *et al*., 1997). The reaction was carried out in the presence of 10 μM $CaCl_2$ and 2 nM protein as these have been shown earlier to be the optimum concentration for activation of EhCaBP1-dependent protein kinase(s). The result is shown in Fig. 10. There was a marked reduction (60%) in the ability of the mutant to activate kinase(s) as compared with the WT EhCaBP1 suggesting that activation of the kinase may require the ability of EhCaBP1 to bind Ca^{2+}.

(A)

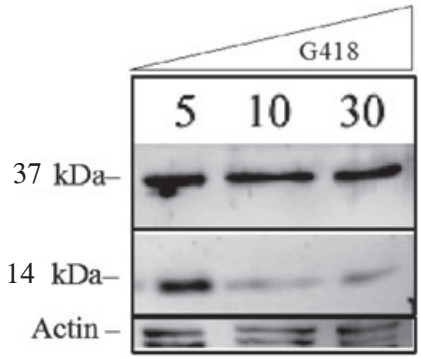

(B)

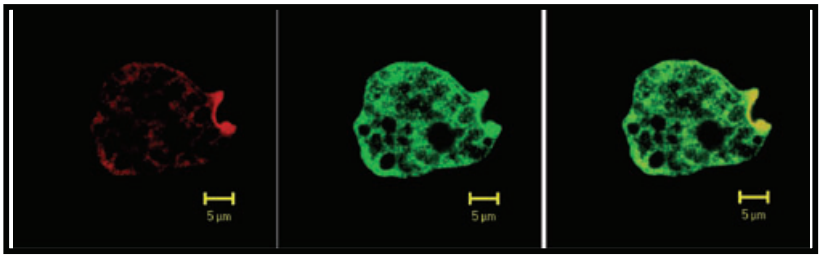

(C)

(i)

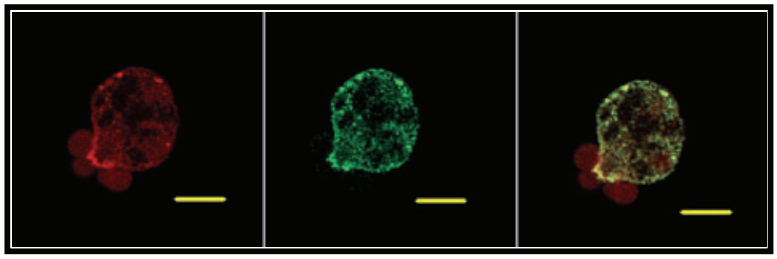

(ii)

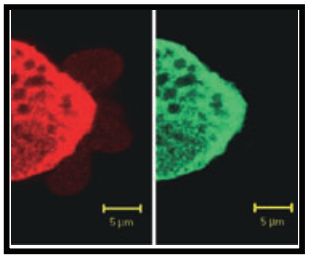

(D)

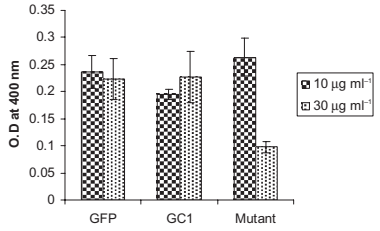

(E)

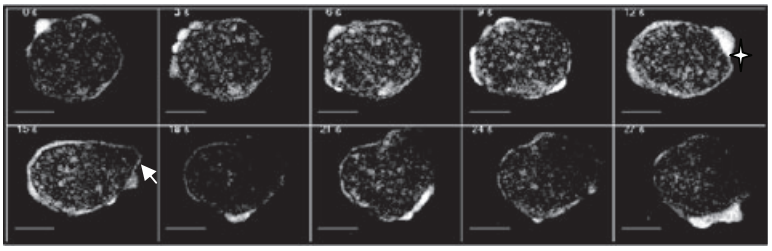

Fig. 8. Expression and localization of CaBP1ΔEF in *E. histolytica* during erythrophagocytosis.
A. GFP-CaBP1ΔEF-expressing cells were maintained at different G418 concentrations (5, 10, 30 μg ml^{-1}). Fifty micrograms of the lysate was used for Western blotting and immunolocalization using anti-EhCaBP1 antibody. The blots were stripped and re-probed with anti-Ehactin antibody. Anti-EhCaBP1 antibody stains both the endogenous EhCaBP1 band at 14 kDa and the GFP-fused EhCaBP1ΔEF band at 37 kDa.
B–C. GFP-CaBP1ΔEF during erythrophagocytosis was visualized by immunolocalization in cells expressing GFP-CaBP1ΔEF at 10 μg ml^{-1} G418 (B) or 30 μg ml^{-1} G418 (C, i, ii). The slides were prepared as described in *Experimental procedures*. GFP-CaBP1ΔEF was stained with anti-GFP antibody (green) and phalloidin (red) and viewed using CSLM. (C, i) Confocal section of a representative cell; (C, ii) an enlarged view of the membrane of a cell. RBC binding to the surface and the colocalization of GFP-CaBP1ΔEF and F-actin are clearly visible.
D. Erythrophagocytosis in cells expressing high level of mutant protein. The cells expressing GFP-CaBP1ΔEF, GFP-EhCaBP1 (GC1) or vector alone (GFP) were grown at 10 μg ml^{-1} and 30 μg ml^{-1} G418. Erythrophagocytosis was measured after incubating 10^5 amoebae with 10^7 RBC for 10 min at 37°C. The level of haem was determined by measuring absorbance at 400 nm which was a direct estimate of the ingested RBC. The histogram shows relative mean optical density ± SD of three independent experiments.
E. The micrograph represents a time sequence of a motile trophozoite expressing GFP-CaBP1ΔEF. Acquisitions were performed as for the GC1 cells expressing WT EhCaBP1. The analysis and the three-dimensional reconstruction was performed as described above. Bar represents 10 μm. Note the accumulation of GFP-CaBP1ΔEF in the protrusions (star) and the fast disappearance (arrow) as the cell moves.

Discussion

Entamoeba histolytica has an extensive signalling system unlike many other protozoan parasites. The extent of the signalling network can be gauged by the fact that this microorganism has a large repertoire of novel CaBPs and *trans*-membrane kinases (Loftus *et al*., 2005; Bhattacharya *et al*., 2006). The function of most of these molecules in amoebic biology has not been studied except for EhCaBP1. It has been implicated in cellular processes associated with dynamic membrane-cytoskeletal structures involving actin remodelling, such as pseudopod formation and phagocytosis (Sahoo *et al*., 2004). Normally Ca^{2+} signalling is mediated through CaBPs, many of which are Ca^{2+} sensors and participate in downstream signal transduction processes and are known to carry out diversity of functions (Berridge *et al*., 2000).

The results presented here clearly showed that EhCaBP1 is a highly dynamic molecule and it associates transiently with subcellular assemblies, such as actin filaments, mostly in the initial stages when the phagocytic cups or pseudopods are being formed. Interestingly, it was also observed using a mutant protein defective in Ca^{2+} binding (CaBP1ΔEF) that this association of EhCaBP1 with actin filaments in the formation of phagocytic cups may not have a strict requirement for its ability to bind Ca^{2+}. It is unlikely that full functional property of EhCaBP1 is due to little residual Ca^{2+}-binding activity of CaBP1ΔEF, as the presence of low-affinity binding sites in EhCaBP1 and the residual binding does not change conformation in the presence of Ca^{2+} (Moorthy *et al*., 2001). There are very few examples where the functions of CaBPs are independent of their ability to bind Ca^{2+}. Therefore it is significant that the recruitment of EhCaBP1 to the phagocytic cup does not require Ca^{2+} binding. A few other examples are functional complementation of yeast calmodulin by a mutated form of calmodulin with no Ca^{2+} binding ability (Geiser *et al*., 1991), formation of autophagic tubes in a Ca^{2+}-independent manner (Uttenweiler *et al*., 2005) and localization of a flagellar CaBP of *Trypanosoma cruzi* to the flagella in a Ca^{2+}-independent manner (Buchanan *et al*., 2005).

Phagocytosis is a crucial activity for the survival and virulence of *E. histolytica* (Orozco *et al*., 1983). Although a number of studies have been carried out, there is still no clear understanding of the molecular mechanisms involved in the process which start with the binding on the amoebic surface of the target cell. The signalling upon binding triggers the formation of a phagocytic cup leading to actin filaments re-organization. Closure of this cup ends with the formation of an early phagosome that maturates to fuse with lysosomes. Proteomic strategy has been primarily used to identify the molecules present in early phagosomes (Marion *et al*., 2005; Okada *et al*., 2005). However, EhCaBP1 was not found in the phagosome proteome, in spite of its clear involvement in the process. The absence of EhCaBP1 in the proteome of these phagosomes was in accord with the observation using GFP-tagged EhCaBP1 showing that EhCaBP1 is a highly dynamic molecule and is transiently associated with dynamic ruffling structures (this study). Thus, *in vitro* association of EhCaBP1 and actin filaments demonstrated earlier (Sahoo *et al*., 2004) appears to be transient *in vivo.* The rate of GFP-EhCaBP1 movement during pseudopod formation suggested that the re-organization of EhCaBP1 is a highly rapid process occurring in the initial 3–4 s. The dynamics of EhCaBP1 redistribution during phagocytosis was similar to other actin-associated molecules, such as myosin I (Ostap *et al*., 2003; Marion *et al*., 2004), coronin (Lu and Clarke, 2005), or ER-linked proteins calreticulin and calnexin (Muller-Taubenberger *et al*., 2001). However, for the first time we have shown that a Ca^{2+}-sensing protein, EhCaBP1, undergoes dynamic translocation that correlates with actin filament re-organization during pseudopods extension.

EhCaBP1 was shown to bind both F- and G-actin *in vitro* although with low K_d values (Sahoo *et al*., 2004). This means that EhCaBP1 and actin should normally remain as a complex, with transient composition and stability, according to the need of the cell. From the data presented

(A)

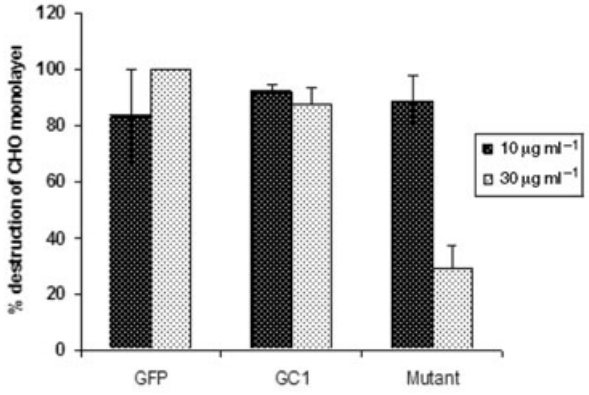

(B)

Transfectant	Cfu ml^{-1}
GFP	0.98 x 10^6
GC1	1.0x10^6
Mutant	0.48 x 10^6

(C)

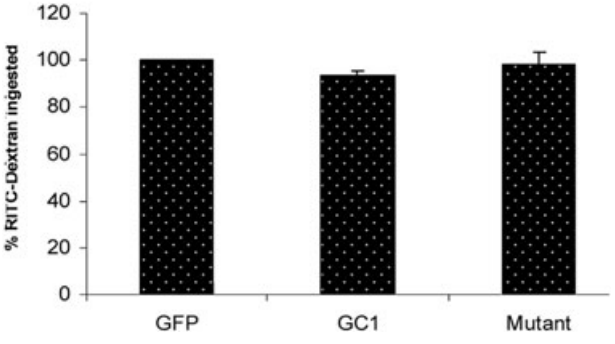

Fig. 9. Properties of cells overexpressing mutant EhCaBP1.
A. Cytopathic assay. The destruction of CHO monolayer by *E. histolytica* cells (GFP-CaBP1ΔEF, GFP-EhCaBP1 or GFP) was determined as described in *Experimental procedures*. The cells were grown at 10 or 30 μg ml^{-1} G418 for 48 h as indicated.
B. Bacterial uptake. The uptake of bacteria (*E. coli*) ingested by GFP, GFP-CaBP1ΔEF or GFP-EhCaBP1 cell lines, grown at 30 μg ml^{-1} for 48 h was determined as described in *Experimental procedures*. The uptake was expressed as cfu ml^{-1}.
C. Fluid-phase endocytosis. The cells expressing GFP-CaBP1ΔEF, GFP-EhCaBP1 (GC1) or vector alone (GFP) were grown at 30 μg ml^{-1} G418 for 48 h as described. The cells were then incubated with 2 mg ml^{-1} RITC-dextran in PBS for 30 min and intracellular fluorescence was measured using spectrofluorimeter as described in *Experimental procedures*. The histogram shows relative mean intensity ± SD of three independent experiments.

here, it is difficult to conclude on the role of EhCaBP1 and G-actin interaction *in vivo* if any. In contrast during phagocytosis, the colocalization of EhCaBP1 with F-actin *in vivo* correlates with the *in vitro* findings and suggests that EhCaBP1 and F-actin interaction should be postulated as an important event in the process of cytotoxicity and phagocytosis of human cells by *E. histolytica*.

The target cell killing by *E. histolytica* requires parasite cell recognition at their surface and triggering of appropriate signal that leads to cell death. It is also thought that RBC on binding to the cell surface might trigger a unique signal which activates a signalling cascade leading to the formation of a phagocytic cup and finally RBC engulfment. We observed a defect in phagosome formation in cells overexpressing CaBP1ΔEF mutant, defective in its ability to bind Ca^{2+}. Although CaBP1ΔEF localizes to the phagocytic cups, RBC uptake and target cell killing were highly impaired in cells overexpressing this Ca^{2+}-insensitive mutant of EhCaBP1. The data thus indicate that Ca^{2+} binding is not required by EhCaBP1 to initiate phagocytosis or to be recruited at the phagocytic cup at early stages of phagocytosis. The transient behaviour of EhCaBP1 at the phagocytic cup may, therefore, be regulated by other accessory factors, influencing stability of EhCaBP1 interaction with F-actin. It is likely that the defect in closure and phagosome maturation observed in cells overexpressing the mutant protein may be a result of a dominant negative effect of the mutant form potentially sequestering these EhCaBP1 partners. This phenotype may also be due to the reduced ability of the mutant EhCaBP1 (hence early located to the phagocytic cup) to interact or activate downstream targets through Ca^{2+}-dependent mechanism leading to phagosome closure and maturation. Although not much information is available regarding the molecular mechanism of phagosome maturation in *E. histolytica*, the role of kinases has been documented (Batista Ede and de Souza, 2004). For instance, although the specific EhCaBP1 target protein kinase(s) has not been identified so far it was shown before that *E. histolytica* cells have a protein kinase that can be activated by EhCaBP1 (Yadava *et al.*, 1997). The EhCaBP1 mutant protein has reduced ability to activate this unknown kinase(s). Overexpression of CaBP1ΔEF mutant also resulted in reduction of parasite cytotoxicity, a phenotype not yet explored. However, the data encourage us to postulate a downstream signal transduction pathway depending on EhCaBP1 bound to Ca^{2+} as a mechanism for initiating target cell killing.

We should conclude that EhCaBP1, like other CaBPs, is likely to have multiple targets and binding to some of the targets may not require Ca^{2+} while some may. Future studies are focusing on unravelling the nature of this downstream signalling pathway initiated by EhCaBP1.

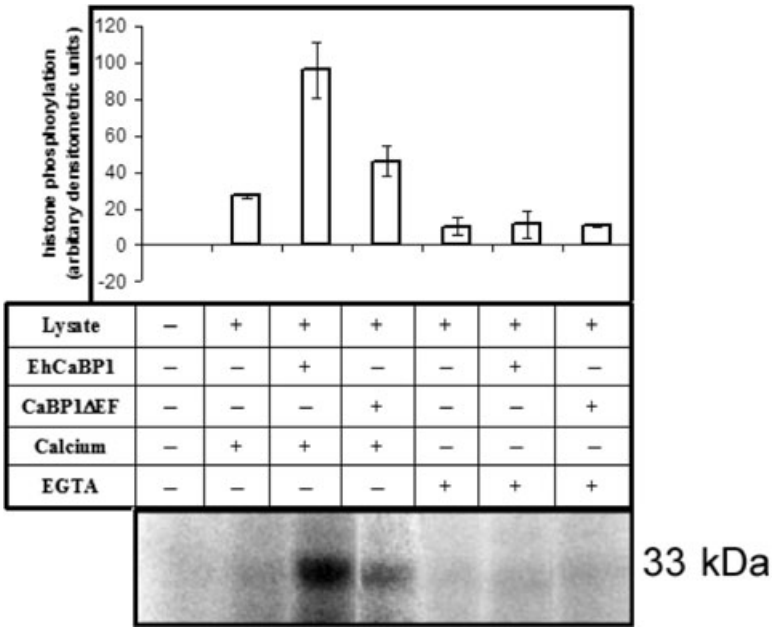

Fig. 10. Reduced activation of kinase(s) by CaBP1ΔEF. *E. histolytica* cell-free lysate (25 μg) was used as the source of kinase and histone type III (15 μg) as the substrate. EhCaBP1 and CaBP1ΔEF were used for the assay at 2 nM. The concentration of Ca^{2+} used was 10 μM. The assay was performed as described in *Experimental procedures* using [γ-^{32}P]-ATP as the phosphate donor. The reaction products were separated on a 12% SDS-PAGE and the amount of radioactivity incorporated into histone was determined by densitometry. The graph represents the histogram of the various reactions, as indicated in the table ±SD of three independent experiments. The lowest panel depicts a representative gel picture. The first lane in all cases is histone alone.

Experimental procedures

Strains and cell culture

Entamoeba histolytica strain HM1:IMSS clone 6 was maintained and grown in TYI-S-33 medium containing 125 μl of 250 U ml^{-1} Benzyl Penicillin and 0.25 mg ml^{-1} Streptomycin per 100 ml of medium. Neomycin (Sigma) was added at 10 μg ml^{-1} for maintaining transgenic cell lines.

Intracellular Ca^{2+} measurements

Trophozoites (10^6) were washed twice with PBS and loaded with 20 μM FURA 2-AM (Sigma Chemicals) at room temperature in the dark for 1 h in buffer A (20 mM Hepes, pH 7.2, 140 mM NaCl) supplemented with 0.1% BSA. Loaded cells were washed twice with PBS and re-suspended in buffer A. Cells were transferred to a thermostated fluorometric cuvette containing a magnetic stir bar and maintained at 37°C with gentle agitation. BAPTA-AM was added directly to the cuvette. Fluorescence values were registered in a Cary Fluorescence Spectrophotometer, programmed to obtain the emission at 510 nm on excitation at 340 and 380 nm simultaneously. $[Ca^{2+}]_i$ is represented as the 340–380 nm ratio as these are considered proportional to each other (Grynkiewicz *et al*., 1985).

Cloning of EhCaBP1 gene in pEh-NEO-GFP vector

Primers to amplify the EhCaBP1 were designed based on the *Entamoeba* genome sequence database. BamHI restriction site was incorporated in both the primers. The primers used were GC1-F, 5′-GGGGGATCCCATATGGCTGAAGCACT-3′ and GC1-R, 5′-GGGGGATCCAGTTTAGAGTGAAAACT-3′. An amplicon of 405 bp was obtained by PCR amplification. It was cloned in the BamHI site of the pEh-NEO-GFP vector downstream to GFP gene. The vector has been previously constructed (N. Guillen, unpublished) by cloning the GFP mut3 allele of GFP (Cormack *et al*., 1996) in the unique BamHI site of the pExEhNeo plasmid (Hamann *et al*., 1995). The different constructs (GC1 or vector) were used to transform *Escherichia coli* strain DH5α cells following standard methods.

Transfection and selection of E. histolytica *trophozoites*

Transfection of *E. histolytica* cells by pEhNEO/GC1 DNA was performed by electroporation as described previously (Sahoo *et al*., 2003). Briefly, trophozoites in log phase were harvested and washed with PBS followed by incomplete cytomix buffer [10 mM K_2HPO_4/KH_2PO4 (pH 7.6), 120 mM KCl, 0.15 mM $CaCl_2$, 25 mM Hepes, 2 mM EGTA, 5 mM $MgCl_2$]. The washed cells were then re-suspended in 0.8 ml of complete cytomix buffer (incomplete cytomix containing 4 mM Adenosine Triphosphate, 10 mM Glutathione) containing 200 μg of plasmid DNA and subjected to two consecutive pulses of 3000 V cm^{-1} (1.2 kV) at 25 μF (Bio-Rad, electroporator). The transfectants were initially allowed to grow without any selection. Drug selection was initiated after 2 days of transfection in the presence of 10 μg ml^{-1} G418 (Sigma).

Immunofluorescence staining

Immunofluorescence staining was carried out as described before (Sahoo *et al*., 2004). Briefly, *E. histolytica* cells were allowed to adhere on to a glass coverslip for 5 min at 37°C in TYI-33 medium. RBC was added to the cells for indicated time at the ratio of 10 RBC per cell. Phagocytosis was stopped by fixation in 3.7% PFA for 30 min. The cells were then incubated in 50 mM NH_4Cl for 30 min before permeabilization with 0.1% Triton X-100 for 1 min. Non-specific sites were blocked by incubation with 1% BSA/PBS for 30 min at 37°C. While actin was labelled by Phalloidin-TRITC (1/500) both GFP and EhCaBP1 were identified by respective antibodies (GFP at 1:200, Molecular probes; EhCaBP1 at 1:30). The bound antibodies were visualized by

anti-rabbit secondary antibodies coupled with Alexa 488 (1/200) or Cy3 (1/300) (Molecular Probes). The preparations were further washed with PBS and mounted on a glass-slide using DABCO [1,4-diazbicyclo (2,2,2) octane, Sigma, 10 mg ml^{-1} in 80% glycerol]. Sealing of the coverslip edges was performed with nail-paint to avoid drying.

Confocal laser scanning microscopy

Fluorescent samples were examined on an LSM 510 confocal laser scanning microscope (Zeiss, Germany) equipped with a 63× objective. Alexa-red-labelled samples were visualized after excitation at 543 nm using He/Ne Laser and Alexa-green-labelled samples after excitation at 488 nm using Argon Laser. Focal planes of 0.8 μm sections with a shift of objective by 1 μm were captured for about 20 planes from the bottom to the top of each cell. Images were processed using LSM 510 software, Zeiss, Germany.

Time-lapse imaging

The cells expressing GFP-CaBP1, GFP-CaBP1ΔEF or GFP alone were plated onto a 35 mm Mat Tek glass bottom culture dish (Mat Tek Corporation) at 37°C. After the cells got settled at the bottom, the medium was removed and the glass chamber was filled with pre-warmed PBS. The dish was kept on a platform with a temperature controller (Tempcontrol 37-2 digital, Zeiss) to maintain temperature at 37°C. High-resolution fluorescent time-lapse imaging of a moving and phagocytosing amoeba was performed using a high-speed spinning disk confocal system (UltraView RS, Perkin Elmer) equipped for axial *z*-stack sampling throughout the cell volume. This system was attached to an inverted 200 M microscope (Zeiss). The images were captured with an Orca D-ER detector (Hamamatsu) and a 40× objective and 2 × 2 binning. Images of 1.5 μm (along *z*-axis) at 3 or 4 s interval (as indicated) were captured. This *z*-spacing was optimized to: (i) monitor the entire depth of amoeba from top to bottom and (ii) accomplish fast capturing of a moving amoeba. The raw images were processed using ImageJ software available freely on the web (http://rsb.info.nih.gov/ij/). For each time point, raw images were three-dimensionally reconstituted before further analysis.

Image analysis

Raw images obtained from the microscope were processed and analysed using Image J software (Plugins/PE_raw/Convert files to tiff series) and the three-dimensional images were reconstructed (Images/Stacks/Z project) by taking standard deviation of the selected slices and projected as a time series. For quantitative measurements of the pseudopods, the time point just before the pseudopod protrusion was referred to as t = 0. The measurement of grey scale intensity of the images was performed as described elsewhere (Aizawa *et al*., 1997).

Generation of CaBP1ΔEF mutant

EhCaBP1 mutants were generated using a site-directed mutagenesis kit (Stratagene, La Jolla, CA). The protocol followed was essentially as described by the manufacturer. The first aspartate (D) residue of each EF hand was mutated to alanine (A) residue. The mutations were performed in a sequential order one residue at a time. The modified amplicon was used as a template for the next round of mutation to get a mutant having all the four D mutated to A (CaBP1ΔEF). The mutations were confirmed by nucleotide sequencing. The primers used were

EFI F: 5′-CTTTTTAAAGAAATTGCAGTTAATGGAGATGGAG-3′
EFI R: 5′-CTCCATCTCCATTAACTGCAATTTCTTTAAAAAG-3′
EFII F: 5′-CAAATCTATTGCAGCTGATGGAAA-3′
EFII R: 5′-TTTCCATCAGCTGCAATAGATTTG-3′
EFIII F: 5′-CTATAAACTTATGGCAGTTGATGGAGATGG-3′
EFIII R: 5′-CCATCTCCATCAACTGCCATAAGTTTATAG-3′
EFIV F: 5′-GTTATGAAAGCTGCAGCTAATGGTGATG-3′
EFIV R: 5′-CATCACCATTAGCTGCAGCTTTCATAAC-3′

Expression and purification of recombinant proteins in E. coli

The purification of all the recombinant proteins (WT and mutants) was carried out essentially as for WT EhCaBP1 (Prasad *et al*., 1993).

Circular dichroism spectroscopy

CD measurements were performed using a Jasco-815 spectropolarimeter. Each spectrum was measured in the far-UV region (200–260 nm) and was an average of five scans. Scans were performed at a protein concentration of 33 μM (50 mM Tris·Cl, pH 7.0 and 100 mM NaCl) using a cuvette of path length 1.0 cm in the presence of 5 mM $CaCl_2$. Percentage helical content was calculated using the method described by Barrow *et al*. (1992).

Isothermal calorimetry

Isothermal calorimetry measurements were performed with a Microcal Omega titration calorimeter at 25°C. Samples were centrifuged and degassed prior to the titration. A typical titration consisted of injecting 2 μl aliquots of 20 mM Ca^{2+} solution (diluted from 1 M standard $CaCl_2$ solution supplied from Sigma-Aldrich chemicals) into 200 μM protein solution after every 3 min to ensure that the titration peak returned to the baseline prior to the next injection. A total of 70 injections were carried out. Aliquots of concentrated ligand solution were injected into the buffer solution (without the protein) in a separate ITC run, to subtract the heat of dilution. Two sets of titrations were carried out: (i) apo-EhCaBP1 in 50 mM Tris·Cl, pH 7.0 and 100 mM NaCl and (ii) apo-CaBP1ΔEF in 50 mM Tris·Cl, pH 7.0 and 100 mM NaCl. The ITC data were analysed using the software ORIGIN (supplied with Omega Microcalorimeter). The amount of heat released per addition of the titrant was fitted to best least squares fit model as given by Wiseman *et al*. (1989).

Actin and CaBP1ΔEF co-sedimentation assay

Co-sedimentation assay was carried out following published conditions (Sahoo *et al*., 2004). Briefly, 5 μM of rabbit muscle G-actin (Sigma) was polymerized for 60 min in polymerization buffer

containing 100 mM KCl and 2 mM $MgCl_2$ at room temperature. After polymerization, actin was mixed with 1 mM ATP and appropriate target protein (5 μM) in a total volume of 150 μl of G-buffer (10 mM Tris-Cl, pH 7.5, 2 mM $CaCl_2$, 2.5 mM β-Mercaptoethanol, 0.5 M KCl, 10 mM $MgCl_2$) and incubated for 2 h at room temperature. The samples were centrifuged at 100 000 *g* for 45 min at 4°C. The supernatant (one-fourth of total) and pellet fractions (total) were analysed by 15% SDS-PAGE followed by Coomassie blue staining. In addition to CaBP1ΔEF, WT EhCaBP1 and EhCaBP2 were also used as positive and negative controls respectively.

Solid-phase assay

Different wells of a 96-well plate were coated with 5 μM G-actin in PBS overnight at 4°C and were blocked with 3% BSA in PBS for an additional 24 h. After washing with PBS-T (PBS containing 0.05% Tween-20), EhCaBP1 and CaBP1ΔEF were added to the wells in duplicates at concentrations ranging from 1.4 μM to 5 μM. Bound protein was detected with anti-EhCaBP1 antibody followed by HRPO-linked anti-rabbit IgG using the colorimetric substrate TMB (Sigma). The absorbance was monitored at 405 nm with a microplate reader (Bio-Rad, USA) after stopping the reaction with 2 N H_2SO_4. The reaction was carried out in the presence of 5 mM $CaCl_2$ or 2 mM EGTA as indicated.

Phagocytosis of RBC by trophozoites

To quantify the RBC ingested by amoebae, the colorimetric method of estimation was followed as described earlier (Sahoo *et al*., 2004). Briefly, RBC washed with PBS and TYI-33 medium were incubated with amoebae for indicated time at 37°C in 0.2 ml of culture medium at a ratio of 100:1 (RBC:Amoeba). To test the effect of BAPTA-AM on erythrophagocytosis, amoeba were initially treated with the specified concentrations of BAPTA-AM at room temperature for 10 min and then incubated with RBC. The amoebae and erythrocytes were pelleted down and non-engulfed RBC were lysed with cold distilled water and centrifuged at 1000 *g* for 2 min. This step was repeated twice, followed by re-suspension in 1 ml formic acid to burst amoebae containing engulfed RBC. The optical density of the samples was determined by a spectrophotometer at 400 nm using formic acid as blank.

Cytopathic assay

The destruction of monolayer of CHO cells was assayed as described by Bracha and Mirelman (1984). Briefly, trophozoites (10^5 ml^{-1} suspended in DMEM without FCS) were added in triplicate to wells containing a confluent monolayer of CHO cells (10^5 ml^{-1}) pre-washed with DMEM to remove traces of fetal calf serum and incubated for 60 min at 37°C in an atmosphere of 95% air and 5% CO_2. The reaction was stopped by chilling for 10 min and the wells were then washed thrice with cold PBS. The monolayer was fixed with 4% paraformaldehyde for 10 min and stained with methylene blue (0.1% in borate buffer, 0.1 M, pH 8.7). The excess stain was washed with 0.01 M borate buffer and the incorporated dye was extracted by adding 1.0 ml of 0.1 M HCl at 37°C for 30 min. The colour was read in a spectrophotometer at 660 nm after appropriate dilutions with 0.1 M HCl. Destruction of cells was expressed in relation to the amount of dye extracted from the control monolayer of CHO cells.

Bacterial uptake assay

Bacterial uptake by *E. histolytica* transfectants was determined by measuring the number of bacteria ingested [colony-forming units (cfu) ml^{-1}]. Briefly, 10^5 amoebae were incubated with 10^7 bacteria (*E. coli*) at 37°C for 15 min in a volume of 200 μl. The mixture was centrifuged at 300 *g* for 5 min to pellet only the amoeba and not the non-engulfed bacteria. Amoebae were then washed with PBS three times and then re-suspended in PBS containing 0.1% Triton X-100. The ingested bacteria were pelleted by centrifugation and washed with PBS (thrice) to remove traces of the detergent. The number of bacteria was then determined by plating on LB-Agar plates at different dilutions.

RITC-dextran uptake analysis

The pinocytosis of *E. histolytica* was studied by observing the uptake of RITC-dextran as described before (Sahoo *et al*., 2004). The mid-log-phase cells were harvested, washed and re-suspended in fresh medium. The washed cells were then incubated with RITC-dextran (2 mg ml^{-1}, Sigma) for 30 min at 36°C followed by harvesting and washing with PBS. The cells were then re-suspended in PBS containing 0.1% Triton X-100. The amount of pinocytosed particles was determined by measurement of total fluorescence using a Cary Fluorescence Spectrophotometer.

In vitro *kinase assay*

Total *Entamoeba* cell extract was prepared and the activity of EhCaBP1-dependent kinases was estimated according to Chandok and Sopory (1992). The reaction mixture contained 30 mM Hepes, pH 7.5, 5 mM $MgCl_2$, 15 μg of Histone (Type IIIS, Sigma), 25 μg of *E. histolytica* cell extract, protease inhibitor cocktail, $CaCl_2$ or EGTA. Either EhCaBP1 (2 nM) or CaBP1ΔEF (2 nM) was also added. The reaction volume was adjusted to 40 μl. The reaction was initiated by adding 100 μM [γ-^{32}P]-rATP (specific activity 5000 Ci $mmol^{-1}$, BRIT) and allowed to proceed at 30°C for 20 min. The reaction was terminated by adding 1× SDS-PAGE buffer and resolved on a 12% SDS-PAGE. The gels were dried and exposed to an X-ray film or an imaging plate.

Western analysis

For immunodetection, samples were separated on a 12% or a 15% SDS-PAGE as indicated. The gel was then transferred to a nitrocellulose membrane by semidry method and processed using standard methods. The antigens were detected with polyclonal anti-GFP (1:2000, Molecular probes) or anti-EhCaBP1 (1:1000, Sahoo *et al*., 2004) and with anti-Rabbit HRPO (1:10 000, Amersham). ECL reagents were used for visualization (Amersham). Actin was detected using anti-Ehactin (raised in our laboratory) at 1:1000 dilution.

Acknowledgements

We gratefully acknowledge Spencer Shorte and Pascal Roux from the Imagopole at Pasteur Institute for assistance and

support in the imaging experiments. This work was partially supported by grants from the Department of Biotechnology and CSIR, Government of India. This work was also supported by Grant INCO-DEV in the Fifth Framework Program of the European Union to Nancy Guillén. R.J. thanks UGC, India for Junior and Senior Research Fellowships and French Embassy, New Delhi for the travel grants and fellowship.

References

Aizawa, H., Fukui, Y., and Yahara, I. (1997) Live dynamics of *Dictyostelium cofilin* suggests a role in remodeling actin latticework into bundles. *J Cell Sci* **110** (Part 19)**:** 2333–2344.

Atreya, H.S., Sahu, S.C., Bhattacharya, A., Chary, K.V., and Govil, G. (2001) NMR derived solution structure of an EF-hand calcium-binding protein from *Entamoeba histolytica*. *Biochemistry* **40:** 14392–14403.

Barrow, C.J., Yasuda, A., Kenny, P.T., and Zagorski, M.G. (1992) Solution conformations and aggregational properties of synthetic amyloid beta-peptides of Alzheimer's disease. Analysis of circular dichroism spectra. *J Mol Biol* **225:** 1075–1093.

Batista Ede, J., and de Souza, W. (2004) Involvement of protein kinases on the process of erythrophagocytis by *Entamoeba histolytica*. *Cell Biol Int* **28:** 243–248.

Berridge, M.J., Lipp, P., and Bootman, M.D. (2000) The versatility and universality of calcium signalling. *Nat Rev Mol Cell Biol* **1:** 11–21.

Bhattacharya, A., Padhan, N., Jain, R., and Bhattacharya, S. (2006) Calcium-binding proteins of *Entamoeba histolytica*. *Arch Med Res* **37:** 221–225.

Bracha, R., and Mirelman, D. (1984) Virulence of *Entamoeba histolytica* trophozoites. Effects of bacteria, microaerobic conditions, and metronidazole. *J Exp Med* **160:** 353–368.

Buchanan, K.T., Ames, J.B., Asfaw, S.H., Wingard, J.N., Olson, C.L., Campana, P.T., *et al.* (2005) A flagellum-specific calcium sensor. *J Biol Chem* **280:** 40104–40111.

Carbajal, M.E., Manning-Cela, R., Pina, A., Franco, E., and Meza, I. (1996) Fibronectin-induced intracellular calcium rise in *Entamoeba histolytica* trophozoites: effect on adhesion and the actin cytoskeleton. *Exp Parasitol* **82:** 11–20.

Chandok, M.R., and Sopory, S.K. (1992) Phorbol myristate acetate replaces phytochrome-mediated stimulation of nitrate reductase in maize. *Phytochemistry* **31:** 2255–2258.

Cormack, B.P., Valdivia, R.H., and Falkow, S. (1996) FACS-optimized mutants of the green fluorescent protein (GFP). *Gene* **173:** 33–38.

De Meester, F., Mirelman, D., Stolarsky, T., and Lester, D.S. (1990) Identification of protein kinase C and its potential substrate in *Entamoeba histolytica*. *Comp Biochem Physiol B* **97:** 707–711.

Geiser, J.R., van Tuinen, D., Brockerhoff, S.E., Neff, M.M., and Davis, T.N. (1991) Can calmodulin function without binding calcium? *Cell* **65:** 949–959.

Gerke, V., Creutz, C.E., and Moss, S.E. (2005) Annexins: linking Ca^{2+} signalling to membrane dynamics. *Nat Rev Mol Cell Biol* **6:** 449–461.

Gopal, B., Swaminathan, C.P., Bhattacharya, S., Bhattacharya, A., Murthy, M.R., and Surolia, A. (1997) Thermodynamics of metal ion binding and denaturation of a calcium binding protein from *Entamoeba histolytica*. *Biochemistry* **36:** 10910–10916.

Gopal, B., Suma, R., Murthy, M.R., Bhattacharya, A., and Bhattacharya, S. (1998) Crystallization and preliminary X-ray studies of a recombinant calcium-binding protein from *Entamoeba histolytica*. *Acta Crystallogr D Biol Crystallogr* **54:** 1442–1445.

Grynkiewicz, G., Poenie, M., and Tsien, R.Y. (1985) A new generation of Ca^{2+} indicators with greatly improved fluorescence properties. *J Biol Chem* **260:** 3440–3450.

Hamann, L., Nickel, R., and Tannich, E. (1995) Transfection and continuous expression of heterologous genes in the protozoan parasite *Entamoeba histolytica*. *Proc Natl Acad Sci USA* **92:** 8975–8979.

Hirata, K.K., Que, X., Melendez-Lopez, S.G., Debnath, A., Myers, S., Herdman, D.S., *et al.* (2007) A phagocytosis mutant of *Entamoeba histolytica* is less virulent due to deficient proteinase expression and release. *Exp Parasitol* **115:** 192–199.

Kumar, S., Padhan, N., Alam, N., and Gourinath, S. (2007) Crystal structure of calcium binding protein-1 from *Entamoeba histolytica*: a novel arrangement of EF hand motifs. *Proteins* **68:** 990–998.

Leavitt, S., and Freire, E. (2001) Direct measurement of protein binding energetics by isothermal titration calorimetry. *Curr Opin Struct Biol* **11:** 560–566.

Lew, D.P., Andersson, T., Hed, J., Di Virgilio, F., Pozzan, T., and Stendahl, O. (1985) Ca^{2+}-dependent and Ca^{2+}-independent phagocytosis in human neutrophils. *Nature* **315:** 509–511.

Loftus, B., Anderson, I., Davies, R., Alsmark, U.C., Samuelson, J., Amedeo, P., *et al.* (2005) The genome of the protist parasite *Entamoeba histolytica*. *Nature* **433:** 865–868.

Lu, H., and Clarke, M. (2005) Dynamic properties of *Legionella*-containing phagosomes in *Dictyostelium amoebae*. *Cell Microbiol* **7:** 995–1007.

Marion, S., Wilhelm, C., Voigt, H., Bacri, J.C., and Guillen, N. (2004) Overexpression of myosin IB in living *Entamoeba histolytica* enhances cytoplasm viscosity and reduces phagocytosis. *J Cell Sci* **117:** 3271–3279.

Marion, S., Laurent, C., and Guillen, N. (2005) Signalization and cytoskeleton activity through myosin IB during the early steps of phagocytosis in *Entamoeba histolytica*: a proteomic approach. *Cell Microbiol* **7:** 1504–1518.

Moorthy, A.K., Singh, S.K., Gopal, B., Surolia, A., and Murthy, M.R. (2001) Variability of calcium binding to EF-hand motifs probed by electrospray ionization mass spectrometry. *J Am Soc Mass Spectrom* **12:** 1296–1301.

Muller-Taubenberger, A., Lupas, A.N., Li, H., Ecke, M., Simmeth, E., and Gerisch, G. (2001) Calreticulin and calnexin in the endoplasmic reticulum are important for phagocytosis. *EMBO J* **20:** 6772–6782.

Okada, M., Huston, C.D., Mann, B.J., Petri, W.A., Jr, Kita, K., and Nozaki, T. (2005) Proteomic analysis of phagocytosis in the enteric protozoan parasite *Entamoeba histolytica*. *Eukaryot Cell* **4:** 827–831.

Orozco, E., Guarneros, G., Martinez-Palomo, A., and Sanchez, T. (1983) *Entamoeba histolytica*. Phagocytosis as a virulence factor. *J Exp Med* **158:** 1511–1521.

Ostap, E.M., Maupin, P., Doberstein, S.K., Baines, I.C., Korn, E.D., and Pollard, T.D. (2003) Dynamic localization of

myosin-I to endocytic structures in Acanthamoeba. *Cell Motil Cytoskeleton* **54:** 29–40.

Prasad, J., Bhattaharya, S., and Bhattacharya, A. (1992) Cloning and sequence analysis of a calcium-binding protein gene from a pathogenic strain of *Entamoeba histolytica*. *Mol Biochem Parasitol* **52:** 137–140.

Prasad, J., Bhattacharya, S., and Bhattacharya, A. (1993) The calcium binding protein of *Entamoeba histolytica*: expression in *Escherichia coli* and immunochemical characterization. *Cell Mol Biol Res* **39:** 167–175.

Ravdin, J.I., Sperelakis, N., and Guerrant, R.L. (1982) Effect of ion channel inhibitors on the cytopathogenicity of *Entamoeba histolytica*. *J Infect Dis* **146:** 335–340.

Ravdin, J.I., Murphy, C.F., Guerrant, R.L., and Long-Krug, S.A. (1985) Effect of antagonists of calcium and phospholipase A on the cytopathogenicity of *Entamoeba histolytica*. *J Infect Dis* **152:** 542–549.

Ravdin, J.I., Moreau, F., Sullivan, J.A., Petri, W.A., Jr, and Mandell, G.L. (1988) Relationship of free intracellular calcium to the cytolytic activity of *Entamoeba histolytica*. *Infect Immun* **56:** 1505–1512.

Sahoo, N., Bhattacharya, S., and Bhattacharya, A. (2003) Blocking the expression of a calcium binding protein of the protozoan parasite *Entamoeba histolytica* by tetracycline regulatable antisense-RNA. *Mol Biochem Parasitol* **126:** 281–284.

Sahoo, N., Labruyere, E., Bhattacharya, S., Sen, P., Guillen, N., and Bhattacharya, A. (2004) Calcium binding protein 1 of the protozoan parasite *Entamoeba histolytica* interacts with actin and is involved in cytoskeleton dynamics. *J Cell Sci* **117:** 3625–3634.

Sahu, S.C., Bhattacharya, A., Chary, K.V., and Govil, G. (1999) Secondary structure of a calcium binding protein (CaBP) from *Entamoeba histolytica*. *FEBS Lett* **459:** 51–56.

Stanley, S.L., Jr. (2003) Amoebiasis. *Lancet* **361:** 1025–1034.

Stendahl, O., Krause, K.H., Krischer, J., Jerstrom, P., Theler, J.M., Clark, R.A., *et al.* (1994) Redistribution of intracellular Ca^{2+} stores during phagocytosis in human neutrophils. *Science* **265:** 1439–1441.

Uttenweiler, A., Schwarz, H., and Mayer, A. (2005) Microautophagic vacuole invagination requires calmodulin in a Ca^{2+}-independent function. *J Biol Chem* **280:** 33289–33297.

Vieira, O.V., Botelho, R.J., and Grinstein, S. (2002) Phagosome maturation: aging gracefully. *Biochem J* **366:** 689–704.

Voigt, H., and Guillen, N. (1999) New insights into the role of the cytoskeleton in phagocytosis of *Entamoeba histolytica*. *Cell Microbiol* **1:** 195–203.

WHO/PAHO/UNESCO report (1997) A consultation with experts on amoebiasis. Mexico City, Mexico 28–29 January, 1997. *Epidemiol Bull* **18:** 13–14.

Wiseman, T., Williston, S., Brandts, J.F., and Lin, L.N. (1989) Rapid measurement of binding constants and heats of binding using a new titration calorimeter. *Anal Biochem* **179:** 131–137.

Yadava, N., Chandok, M.R., Prasad, J., Bhattacharya, S., Sopory, S.K., and Bhattacharya, A. (1997) Characterization of EhCaBP, a calcium-binding protein of *Entamoeba histolytica* and its binding proteins. *Mol Biochem Parasitol* **84:** 69–82.

Supplementary material

The following supplementary material is available for this article online:

Movie S1. The movie represents the time sequence of a moving trophozoite expressing GFP-EhCaBP1. Note the dynamic appearance and disappearance of EhCaBP1 during pseudopod formation and retraction respectively. Bar represents 5 μm.

This material is available as part of the online article from:
http://www.blackwell-synergy.com/doi/abs/10.1111/j.1462-5822.2008.01134.x

Please note: Blackwell Publishing is not responsible for the content or functionality of any supplementary materials supplied by the authors. Any queries (other than missing material) should be directed to the corresponding author for the article.

